

Bifurcation and Chaos of the Memristor Circuit

Wang Zhulin, Min Fuhong, Peng Guangya, Wang Yaoda, Cao Yi

Abstract—In this paper, a magnetron memristor model based on hyperbolic sine function is presented and the correctness proved by studying the trajectory of its voltage and current phase, and then a memristor chaotic system with the memristor model is presented. The phase trajectories and the bifurcation diagrams and Lyapunov exponent spectrum of the magnetron memristor system are plotted by numerical simulation, and the chaotic evolution with changing the parameters of the system is also given. The paper includes numerical simulations and mathematical model, which confirming that the system, has a wealth of dynamic behavior.

Keywords—Memristor, chaotic circuit, dynamical behavior, chaotic system.

I. INTRODUCTION

THE memristor is considered to be the fourth kind of basic circuit elements, in addition to the capacitance, resistance and inductance, and is attracting more and more attention because of its unique characteristics. In 2008, some scientists from the Hewlett-Packard (HP) laboratory announced that a solid state realization of a memristor had been manufactured successfully [1], [2], which proving the famous American Chinese scientist Leon Chua in 1971, who predicted the existence of forth basic circuit element --- memristor [3]. Since the advent of memristors, a great deal of work has been reported in the science field due to their special behaviors. The unique memory function of memristor has begun to attract the attention of scholars, and gradually became the research focus of circuit, materials, biology, and other fields.

Due to its similar nervous system synapses behavior, the circuit simulation of the learning behavior of the foam was carried out by the resistance device in 2009 [4], and successfully mimicked the biological behavior of external environmental stimuli. In 2010, Valsa J. et al. proposed a new flux-controlled memristor circuit model [5], which can be realized with a small number of basic components of HP memristor circuit characteristics, but the model has some disadvantages. For example, the new circuit can only work at lower frequency and does not like a separate two-port elements work directly in other circuits. Currently, the study of the memristor has emerged as a new direction, and penetrated into the neural network [6], [7], basic circuit design, model analysis, and programmable logic [8], etc., and achieved many significant results. Although many researchers are interested in the studying of the SPICE simulation model of the memory

device [9]-[11], very few focus on the new memory circuit model. Nowadays, research in the direction of the resistance is more focused on the theoretical aspect, and the corresponding models in this direction are mostly the piecewise linear [12], [13] and HP actual resistance [14], and the three order nonlinear smooth equation model [15]-[17].

In this work, a type of continuous and smooth model is designed, which is correct by the study of the relationship between the voltage and current phase. Then a new fifth order chaotic circuit with two new memory resistor is designed, and the dimensionless mathematical model is deduced. Through the classical nonlinear circuit analysis method, the dissipativity and stability of the system is studied, and by means of theoretical analysis, numerical simulation, bifurcation diagram and Lyapunov exponent spectrum, we confirm that the system has rich dynamic behavior, and the formation of the circuit has a very important significance in the future engineering application.

II. THE MEMRISTOR MODEL

According to traditional circuit theory, we know that the basic two-terminal circuit elements such as capacitance (C) and resistance (R) and inductance (L) established the four circuit variable correspondence between current (i) and voltage(v) and flux (ϕ) and charge (q), as shown in Fig. 1.

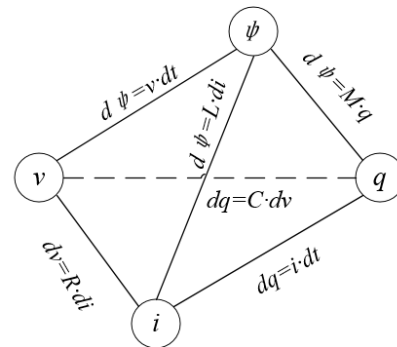


Fig. 1 The basic circuit elements relationship

From Fig. 1, five of the relationships are known to us, but the relationship between (ϕ) and q is not known. Until 1971, Professor Chua defined the incremental resistance $M(q)$ to be the relationship between (ϕ) and q from the perspective of the relationship between the integrity of the circuit variables

$$M(q) = d\phi(q) / dq, \quad (1)$$

which is called a memristor. According to the existing classical circuit theory knowledge

Min Fuhong is Associate Professor, Master Tutor, Research Direction of Chaos Control and Synchronization of Nonlinear System, Nanjing Normal University, China (e-mail: minfuhong@njjnu.edu.cn).

Wang Zhulin is Master Degree, Major in Control Theory and Control Engineering, Nanjing Normal University, China (e-mail: 302576481@qq.com).

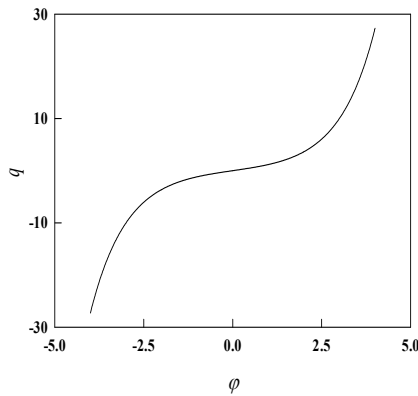
$$\begin{cases} dq = i \cdot dt \\ d\varphi = v \cdot dt, \end{cases} \quad (2)$$

We can obtain $M(q) = v/i$, and the incremental memristive have the same dimension with the resistor. A kind of magnetron memristor characterized by the following nonlinear continuous smooth hyperbolic sine curve is taken as an example to carry out the time-domain analysis of some basic memristive circuits:

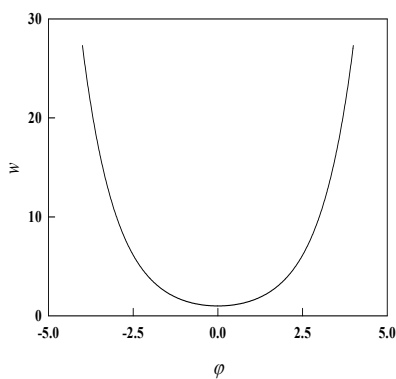
$$q(\varphi) = a \sinh(\varphi), \quad (3)$$

where a is positive real constant, and $q(\varphi)$ is magnetron memristor, and (φ) is the magnetic flux. From (3), the memory conductance model $W(\varphi)$ of the flux-controlled memristor is obtained as:

$$W(\varphi) = \frac{dq(\varphi)}{d\varphi} = \cosh(\varphi). \quad (4)$$



(a) Flux and charge



(b) Flux and memory conductance

Fig. 2 Relationship between flux and charge and memory conductance

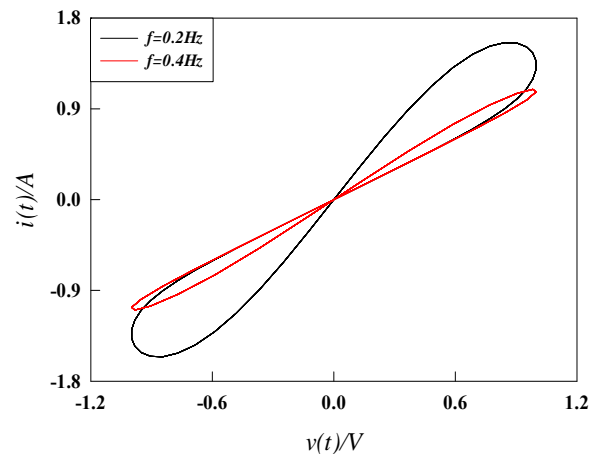
Equation (3) describes the relationship of the magnetron in the plane of the $\varphi - q$ and (4) exhibits the $\varphi - w$. As shown in Fig. 2 (a), it is a monotonic rise of the continuous nonlinear curve. Equation (4) is described by the memory conductance curve

shown in Fig. 2 (b), and the relationship curve is similar to a parabola.

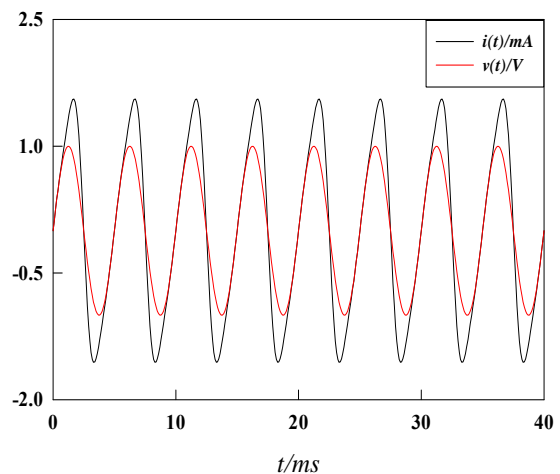
If we set up v and i as the voltage penetrate through the new magnetron memristor model and the current flowing traverse in the new memristor model, respectively. Moreover, if we consider an external sinusoidal voltage stimulus to be imposed across the element, then we will have:

$$\begin{cases} v = \sin(2\pi ft) \\ i = W(\varphi)v = \cosh(y)v \\ d\varphi/dt = v. \end{cases} \quad (5)$$

where π is positive real constant and f is the frequency. The relationship between the voltage and current as displayed in (5) can be simulated by the MATLAB software as shown in Fig. 3, which shows the phase diagram and the time-domain waveform of the voltage and current.



(a) Voltage and current phase diagram



(b) Voltage and current timing diagram

Fig. 3 Relationship between voltage and current

The new memristor describes the same waveform with HP memristor by the relationship of voltage and current, which is

an oblique shape of "8", the compact hysteresis loop shape observed in Fig. 3, and which proves that the memristor model is correct.

III. CHAOS CIRCUIT MODEL CONTAINS WITH TWO MEMRISTORS

In this paper, we design a chaotic circuit including two smooth memristor models, which is shown in Fig. 4.

The new circuit comprises five dynamic components, namely, two capacitors, two resistors and one inductor, and the homologous five state variables are $v_3, v_4, \varphi_1, \varphi_2$ and i_3 , where φ_1 and φ_2 are two internal state variable of memristor. The differential equations of the circuit through the basic voltage

characteristics of each element and Kirchoff's laws can be listed as:

$$\begin{cases} \frac{d\varphi_1}{dt} = v_3, \\ \frac{d\varphi_2}{dt} = \frac{v_4 - v_3}{R_2 W_2 + 1}, \\ \frac{dv_3}{dt} = \frac{1}{C_1} [(G - W_1)v_3 - \frac{W_2}{R_2 W_2 + 1} (v_3 - v_4)], \\ \frac{dv_4}{dt} = \frac{1}{C_2} [\frac{W_2}{R_2 W_2 + 1} (v_3 - v_4) + i_3], \\ \frac{di_3}{dt} = -\frac{1}{L} v_4 - \frac{R_1}{L} i_3. \end{cases} \quad (6)$$

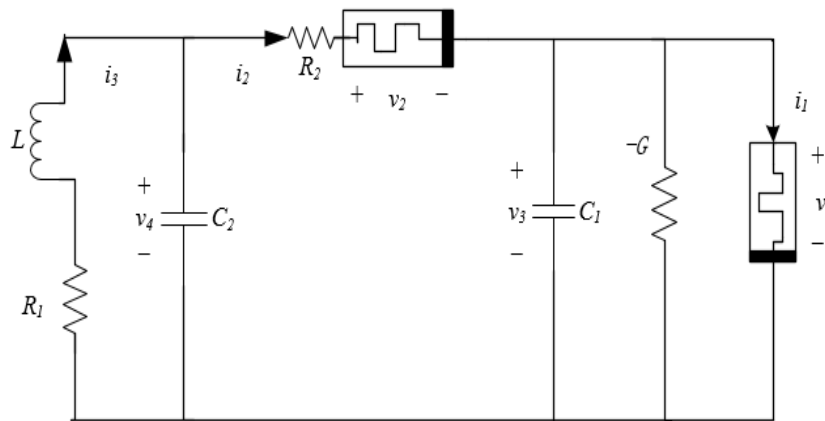


Fig. 4 Containing two memristor chaotic circuit

The values of circuit parameters are $x = \varphi_1, y = \varphi_2, z = v_3, u = v_4, v = i_3, a = 1/C_1, b = 1/L, c = R_1/L, d = G, e = R_2$ and $C_2 = 1$. Two smooth continuous nonlinear function $q(\varphi)$ and $W(\varphi)$ are defined as:

$$\begin{cases} q(\varphi) = \sinh(\varphi) \\ W(\varphi) = \frac{dq(\varphi)}{d(\varphi)} = \cosh(\varphi), \end{cases} \quad (7)$$

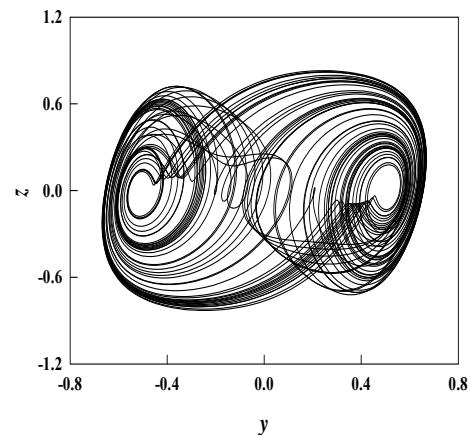
and then (6) can be written as:

$$\begin{cases} \dot{x} = z, \\ \dot{y} = \frac{u - z}{eW_2 + 1}, \\ \dot{z} = a[(d - W_1)z - \frac{W_2}{eW_2 + 1} (z - u)], \\ \dot{u} = \frac{W_2}{eW_2 + 1} (z - u) + v], \\ \dot{v} = -bu - cv. \end{cases} \quad (8)$$

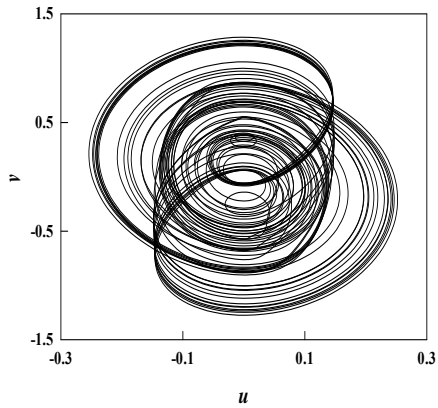
where $W_1 = \cosh(x)$, and $W_2 = \cosh(y)$. Therefore, the new chaotic circuit is a five dimensional system.

IV. THE ANALYSIS OF NEW SYSTEM DYNAMICS

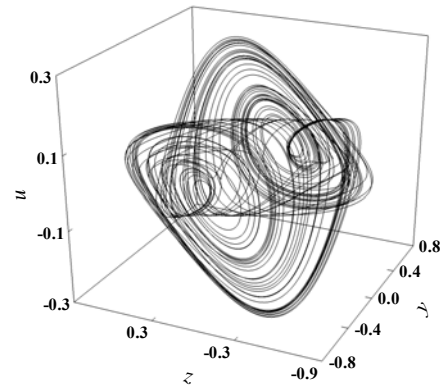
The values of the new system (8) parameters are $a=8, b=10, c=0.01, d=2, e=0.1$ and the initial values of the stated variables are $(0.001, 0, 0.001, 0)$. Fig. 5 exhibits a typical chaotic attractors of the new system, Fig. 6 shows the three-dimensional phase trajectory system of the new chaotic magnetic-controlled memristive circuit. According to the simulation results, the trajectories of system show a complex stretching and twisting structure, but the whole system is stable.



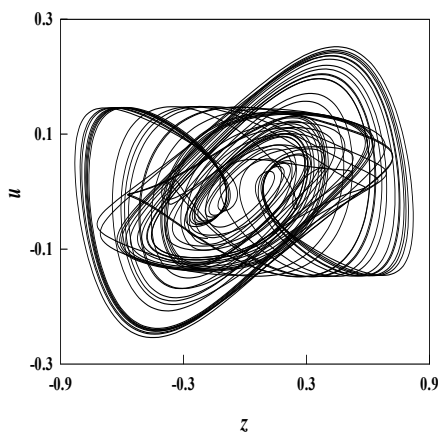
(a) y-z phase locus



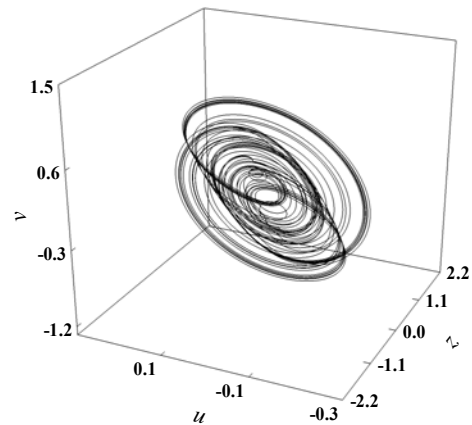
(b) $u-v$ phase locus



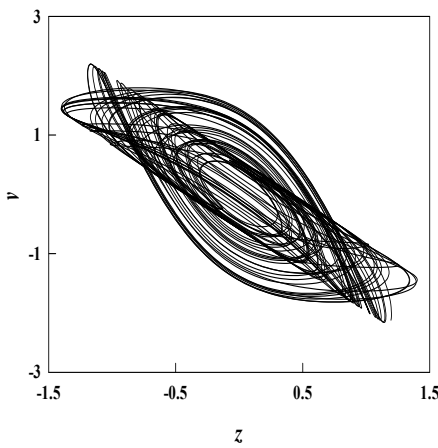
(a) $y-z-u$ phase locus



(c) $z-u$ phase locus



(b) $z-u-v$ phase locus



(d) $z-v$ phase locus

Fig. 6 Three phase locus

A. Dissipation Analysis

The vector field of the new system (8) is given as:

$$\Delta V = \frac{\partial \dot{x}}{\partial x} + \frac{\partial \dot{y}}{\partial y} + \frac{\partial \dot{z}}{\partial z} + \frac{\partial \dot{u}}{\partial u} + \frac{\partial \dot{v}}{\partial v} = -aW_1 - \frac{2W_2}{eW_2 + 1} - c, \quad (9)$$

where W_1, W_2 are positive. The new system is always dissipative with a corresponding exponential contraction rate

$e^{-(aW_1 + \frac{2W_2}{eW_2 + 1} + c)t}$ for any positive value a or c , and in the following exponential convergence:

$$dV / dt = e^{-(aW_1 + \frac{2W_2}{eW_2 + 1} + c)t} \quad (10)$$

That is, a volume element V_0 is contracted by the flow into a volume element $e^{-(aW_1 + \frac{2W_2}{eW_2 + 1} + c)t}$ at time t . In ideal conditions, all the trajectories of the system are in a volume of zero, so that the asymptotic motion can be fixed to an attractor.

B. Equilibrium and Stability Analysis

Let $\dot{x} = \dot{y} = \dot{z} = \dot{u} = \dot{v} = 0$, the balance point of system (8) is given as

Fig. 5 Phase trajectories of the new system

$$A = \{(x, y, z, u, v) | z = u = v = 0, x = l_1, y = l_2\} \quad (11)$$

Each points located on the plane x - y are the balance point of the system, where l_1, l_2 is a real constant. The Jacobi matrix of the new chaotic circuit system(8) can be written as:

$$J_A = \begin{bmatrix} 0 & 0 & 1 & 0 & 0 \\ 0 & 0 & -g & g & 0 \\ 0 & 0 & 8g(2-h_1-h_2) & 8gh_2 & 0 \\ 0 & 0 & gh_2 & -gh_2 & 1 \\ 0 & 0 & 0 & -10 & 0 \end{bmatrix} \quad (12)$$

where $h_1 = \cosh(l_1)$ and $h_2 = \cosh(l_2)$ and $g = 1/(1 + \text{ecosh}(l_2))$, and the characteristic equation are given by:

$$\lambda^5 + a_1\lambda^4 + a_2\lambda^3 + a_3\lambda^2 \quad (13)$$

with

$$\begin{cases} a_1 = 8h_1 + 9gh_2, \\ a_2 = 8gh_1h_2 + 10, \\ a_3 = 80(h_1 + gh_2). \end{cases} \quad (14)$$

According to *Routh-Hurwitz* conditions, when

$$\begin{cases} \Delta_1 = a_1 > 0, \\ \Delta_2 = a_1a_2 - a_3 > 0, \\ \Delta_3 = a_3(a_1a_2 - a_3) > 0, \end{cases} \quad (15)$$

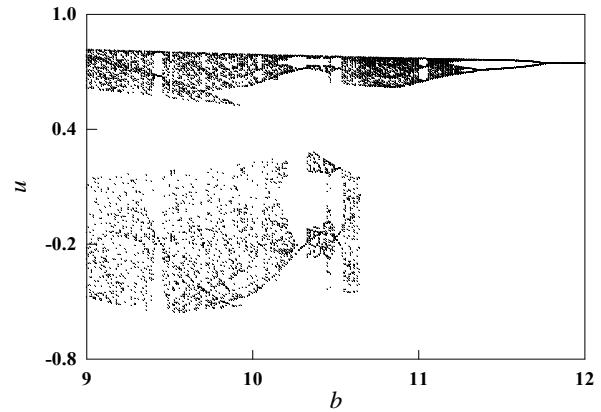
The system real part of the eigenvalue is positive, and then the equilibrium points are unstable and hold the characteristic of a typical magnetic-controlled memristive chaos system. Otherwise, the system will be stable.

C. Bifurcation and Lyapunov spectrum of the System

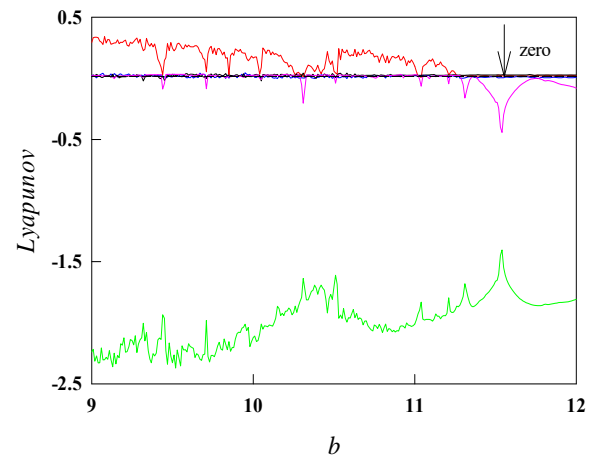
To discuss the complex dynamical behaviors of the new memristor circuit, the Lyapunov spectra and bifurcation diagrams are shown as Fig. 7. With the different parameters of system, the stability of the system will be varied, and the motion state of the system will be changed.

With system parameters $a=8, c=0.01, d=2$ and $e=0.1$, and under initial conditions as $x_0=0.001, y_0=0.001, z_0=0, u_0=0.001, v_0=0$, the bifurcation diagram of the system is shown as Fig. 7 (a), which depicts the nexus between the continuous variable u and the system parameter a , and the Lyapunov exponent spectra with esteem to the parameter a in Fig. 7 (b). If the maximum LE of the system is less than zero, then the system is in periodic motion state. On the other hand, if the maximum LE of the system is greater than zero, then the system will be in a state of chaotic motion. From Fig. 7 (a), we can see that the system is periodic motion in $b \in (11.75, 12)$, and is two periodic motion in $b \in (11.36, 11.75)$. With the parameters decreasing, the system is in four periodic motion in

$b \in (11.27, 11.36)$, and then through period doubling bifurcation again, the system is in eight periodic motion in $b \in (11.25, 11.27)$. Finally, the system is in a chaotic motion for $b < 11.25$. At this time, one of the biggest LE is greater than zero.



(a) Bifurcation diagram

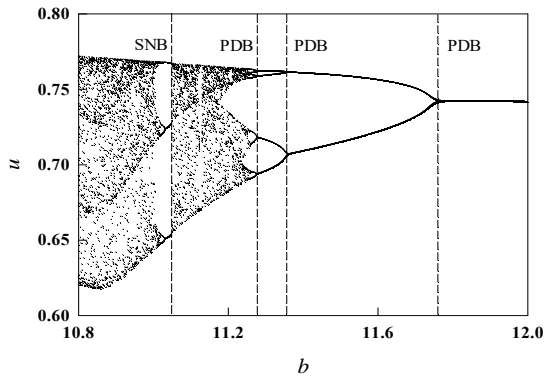


(b) LE spectrum

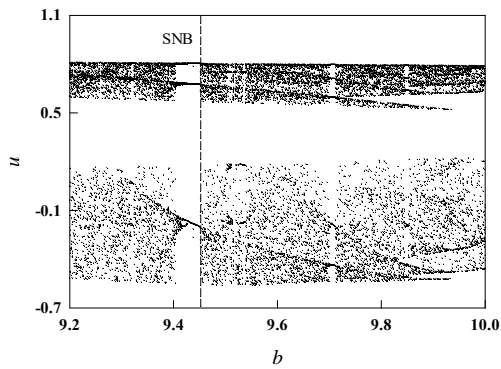
Fig. 7 The bifurcation diagram and Lyapunov exponent spectrum of the new system

To observe the dynamic behavior of the system (8), an enlarged partial bifurcation diagram is given as shown in Fig. 8, in which the numerical simulation step size of 0.005 and the initial values (0, 0.001, 0.001, 00.0001) are given, respectively.

Some ulteriorly specimens of intricate behavior are displayed in Fig. 9. Fig. 9 (a) exhibits a limit cycle with period-1 at $b=15$, and Fig. 9 (b) displays a limit cycle with period-2 at $b=11.6$, and Fig. 9 (c) depicts a limit cycle with period-4 at $b=11.30$, and Fig. 9 (d) shows a limit cycle with period-8 at $b=11.26$, which can also verifiable the bifurcation diagram and LE spectrum of the new system are correct.

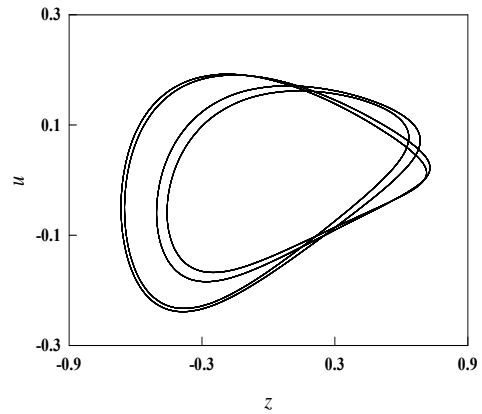


(a) $b \in [10.8, 12]$

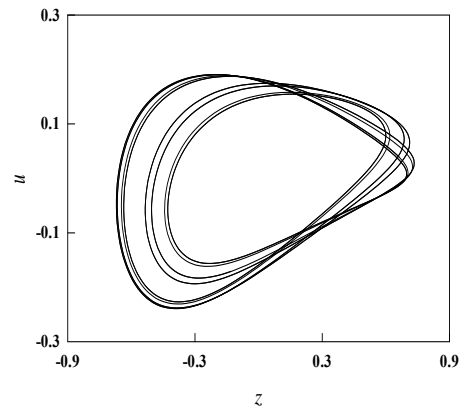


(b) $b \in [9.2, 10]$

Fig. 8 Local bifurcation diagram of the system

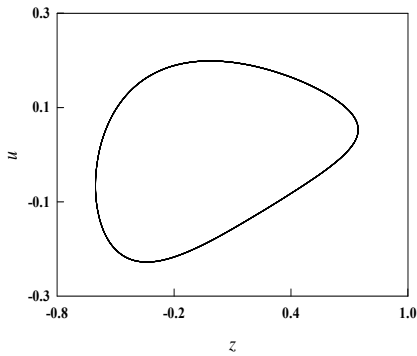


(c) period-4

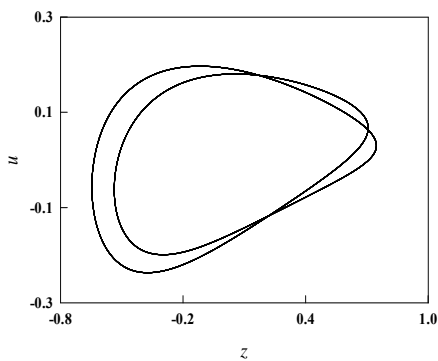


(d) period-8

Fig. 9 Phase diagram of the system for b with different values



(a) period-1



(b) period-2

V. CONCLUSION

In this paper, we designed a magnetron memristor model based on the hyperbolic sine function, and then a memristor chaotic system where the memristor model was proposed. Furthermore, the phase trajectories, the bifurcation diagrams and Lyapunov exponent spectrum of the system were carried out. The numerical simulation results showed that the mathematical model presented in this paper provided a practical magnetron memristor implementation.

ACKNOWLEDGMENTS

The work is supported by the National Natural Science Foundation of China (No. 51475246) and the Natural Science Foundation of Jiangsu Province under Grant No Bk20131402.

REFERENCES

- [1] Strukov D. B., Snider G. S., Stewart D. R., Williams R. S. "The missing memristor found". *Nature*, 2008, vol. 453, pp. 80-83.
- [2] Tour J. M., Tao H. "Electronics: The fourth element". *Nature*, 2008, vol. 453, no. 5, pp. 42-43.
- [3] Chua L. O. "Memristor-the missing circuit element". *IEEE Trans. on Circuit Theory*, 1971, vol. 18, no.5, pp. 507-519.
- [4] Pershin Y. V., La Fontaine S., Di Ventra M. "Memristor model of amoeba learning". *Phys Rev E*, 2009, vol. 80, no. 2, Article ID 21926.

- [5] Valsa J, Biolek D, Biolek Z. "An analogue model of the memristor". *International Journal of Numerical Modeling: Electronic Networks, Devices and Fields*, 2010, vol. 24, no. 4, pp. 400-408.
- [6] Sung Hyun Jo, Ting Chang. "Nanoscale memristor device as synapse in neuromorphic systems". *Nano Lett*, 2010, vol. 10, no.4, pp. 1297-1301.
- [7] Yuriy V. Pershin, Massimiliano Di Bentra. "Experimental demonstration of associative memory with memristive neural networks". *Neural Networks*, 2010, vol. 23, no. 7, pp. 881-886.
- [8] Farnood Merrikh-Bayat, Saeed Bagheri Shouraki. "Memristor based circuits for performing basic arithmetic operation". *Procedia Computer Science*, 2011, vol. 3, pp. 128 -132.
- [9] Fang Xu-Dong, Tang Yu-Hua, Wu Jun-Jie. "SPICE modeling of flux-controlled unipolar memristive devices". *Chin. Phys. B*, 2013, vol. 22, no. 7, Article ID 078901.
- [10] Kai Da Xu, Yong Hong Zhang, Lin Wang, et al. "Two Memristor SPICE Models and Their Applications in Microwave Devices", *IEEE Trans. Nanotechnol.* 2014, vol. 13, no. 3, pp. 607-616.
- [11] Radu Berdan, Chuan Lim, Ali Khiat, Christos Papavassiliou, and Themis Prodromakis, "A memristor SPICE model accounting for volatile characteristics of practical ReRAM", *IEEE Electron Device Lett.* 2014, vol. 35, no. 1, pp. 135-137.
- [12] Iu H. H. C., Yu D. S., Fitch A. L., et al. "Controlling chaos in a memristor based circuit using a Twin-T notch filter". *IEEE Transactions on Circuits and Systems-I: Regular Papers*, 2011, vol. 58, no. 6, pp. 1337 -1344.
- [13] Maheshwar Pd. Sah, Ram Kaji Budhathoki, Changju Yang, et al. "Mutator-Based Meminductor Emulator for Circuit Applications". *Circ. Syst. Signal Pr*, 2014, vol. 33, no. 8, pp. 2363-2383.
- [14] Liu Hai-Jun, Li Zhi-Wei, Yu Hong-Qi, et al. "Memristance Controlling approach based on modification of linear M-q curve". *Chinese Physics B*, 2014, vol. 23, no. 11, Article ID 118402.
- [15] Wei Liu, Fa-Qiang Wang and Xi-Kui Ma. "A unified cubic flux-controlled memristor: theoretical analysis, simulation and circuit experiment". *Int. J. Numer. Model.*, 2015, vol. 28, pp. 335-345.
- [16] Bao Bo-Cheng, Feng Fei, Dong Wei. "The voltage current relationship and equivalent circuit implementation of parallel flux-controlled memristive circuits". *Chin. Phys. B*, 2013, vol. 22, no. 6, Article ID 068401.
- [17] Li Meng-Ping, Xu Xue-Mei, Yang Bing-Chu et al. "A circular zone counting method of identifying a Duffing oscillator state transition and determining the critical value in weak signal detection". *Chin. Phys. B*, 2015, vol. 24, no. 6, Article ID 060504.